

## Dendrites and fronts in a model of dynamical rupture with damage

Didier Sornette and Christian Vanneste

*Laboratoire de Physique de la Matière Condensée, CNRS URA 190, Faculté des Sciences, Université de Nice-Sophia Antipolis, Boîte Postale No. 71, 06108 Nice Cedex 2, France*

(Received 4 April 1994)

Inspired by our previous studies [Phys. Rev. Lett. **68**, 612 (1992); J. Phys. I **2**, 1621 (1992); Phys. Rev. A **45**, 8351 (1992)] for a random system of the antiplane model of dynamical rupture controlled by a damage field (also coined “thermal fuse model” in its electric analog), here, we examine mainly the case of two-dimensional ordered systems (square lattices and continuum), in order to highlight the similarities with and also the differences from other growth phenomena. Two situations are studied: (1) the catastrophic growth of a crack from a nucleus at constant applied stress and (2) the steady-state propagation of a rupture front in a strip under constant applied displacements at the borders. In discrete lattices, numerical simulations of case 1 show a rich “phase diagram” of rupture patterns as a function of the damage exponent  $m$ , with four-leaf-clover-shaped cracks for low  $m$  and dendriticlike cracks with complex sidebranching for larger values of  $m$ . In case 2, the discrete nature of the lattice is at the origin of the observation of many possible coexisting solutions for crack propagation. The case of a one-mesh-thick semi-infinite central crack is solved analytically for its crack tip velocity, which is uniquely determined by a growth criterion involving the history of the damage field at all points ahead of the crack tip. We then present the continuum formulation of the steady-state propagation of a rupture front in a strip under constant applied displacements at the borders, and we find a continuous family of solutions parametrized by the velocity, similar to the Saffman-Taylor problem, which has an infinity of degenerate solutions in the absence of surface tension.

PACS number(s): 64.60.Ht, 05.40.+j, 62.20.Mk

### I. INTRODUCTION

Recently, a simple dynamical version [1] of the electrical fuse model for rupture in random media [2] has been proposed, in which fuses are heated locally by a generalized Joule effect. When its temperature reaches a given threshold, a fuse burns out irreversibly and become an insulator. This thermal fuse model can be considered as an extension of a vast class of models studied in the last few years in the statistical physics community in order to understand the universal feature of rupture in random media. These works have allowed a partial classification of some possible different regimes of rupture [2,3] and in particular have underlined the links between the physics of fracture and fractal growth phenomena [4], thus providing new insight in this field. For example, tensorial elastic fracture in the presence of lattice anisotropy leads to fractal shapes [5] while the corresponding scalar rupture growth gives nonfractal shapes [2,3]. However, these results have been obtained in models in which the evolution of the rupture is *quasistatic*. There is no dynamics but only an irreversible process with no time scale, in the spirit of the growth models such as DLA (diffusion limited aggregation), which describe the *quasistatic* irreversible evolution of complex interfaces [4]. Introducing a dynamics as in our thermal fuse model [1], delay and relaxation effects become important and have been shown to give birth to a wealth of behaviors with fractal crack patterns even in a scalar framework. Interestingly, it was realized that this model (with the special choice of parameters  $m = 1$  and  $a = 0$ , see below) con-

tains the basic physics to describe damage by electromigration of polycrystalline metal films [9].

In this paper, we pursue further the analogies between problems of rupture in statistical models and general growth and propagation phenomena, by pointing out the existence of remarkable similarities between the thermal fuse model [1] and the problem of dendritic solidification on one hand and that of front propagation such as in the Saffman-Taylor finger problem on the other hand [6,7]. Our study is similar in spirits to the attempts of Refs. [8] to identify the roots of complex fractal growth structures in stochastic and random models from the study of ordered systems. Therefore the main thrust of the present paper is in the study of homogeneous systems, containing at most a single initial crack (a notch in the mechanical language) used to initiate the rupture. Much to our surprise, we found an extremely rich phenomenology even in these simple cases where no quenched or annealed disorder is present. Our study presented below suggests ingredients which may be at the origin of the fractal crack structures observed in Ref. [1] for quenched random systems, such as the coexistence and their competition of multiple crack solutions both in discrete lattices and continuum systems, and the existence of some amplification of very small noise near the advancing crack tips and on the crack sides.

In Sec. II, we first recall the definition of our model, both in the electrical and mechanical contexts. We also describe the different regimes. In Sec. III, we first present some results on rupture patterns obtained in weakly disordered systems submitted to a supercritical applied

current (stress) and possessing an initial defect. We observe a dominating role of the initial crack compared to the distributed disorder in controlling the rupture pattern. This led us to the main body of our study which concerns the same problem in homogeneous systems. A remarkably rich “phase diagram” for the rupture patterns is found as a function of the “damage” exponent  $m$ . In Sec. IV we study both a different geometry (strips) and a different excitation [imposed applied voltage (displacements) at the strip borders instead of current (stress)]. Families of solutions for the stable propagation of rupture fronts at constant velocities are found both for discrete and continuous systems. A connection with the Saffman-Taylor problem of a low density fluid pushing a larger density fluid in a channel [6,7] is proposed. Extensive numerical simulations to test these different regimes show that the discrete nature of the lattice dominates the behavior. It is only in the limit of very small damage exponent  $m$  and very large applied voltage that the numerical simulations find rupture patterns obeying the Saffman-Taylor solution with half-strip width crack fronts.

## II. DEFINITION OF THE THERMAL FUSE MODEL AND ITS MECHANICAL ANALOG

### A. Electrical information

Each bond of an  $L$  by  $L$  two dimensional (2D) square lattice of unit mesh oriented at  $45^\circ$  with respect to the two borders is a fuse. The  $45^\circ$  orientation ensures that all bonds play equivalent roles in a homogeneous medium. Furthermore, the maximum current at the tip of a crack is not in general in the direction collinear to the crack but is at  $\pm 45^\circ$ . Periodic boundary conditions are assumed in the direction perpendicular to the two borders which act as bus bars. Some current or voltage is applied on the lattice and the current flows through the system from one bus bar to the other. As in the quasistatic random fuse model [2], the electrical voltages and currents are assumed to have infinitely short response. The current distribution in the network, i.e., the current  $i_n$  in bond  $n$  for all  $n$ , is determined as for a static input current, i.e., by solving the Kirchoff law. In the numerical simulations,

we have used the conjugate gradient technique, with an error criterion  $\epsilon \leq 10^{-20}$ . Once the current in each bond is known, it is reported in the equation giving the time evolution of the  $n$ th fuse temperature  $T_n(t)$ :

$$CdT_n/dt = G_n^{-1}i_n^m - aT_n. \quad (1)$$

This thermal equation is inspired from the physics of a real fuse which burns out by melting. It governs the time evolution of the temperature  $T_n$  of the  $n$ th fuse of specific heat  $C$ , conductance  $G_n = R_n^{-1}$  (with  $G_n$  varying from bond to bond in a disordered systems), and carrying the current  $i_n$ . The first term of the right hand side,  $G_n^{-1}i_n^m$ , accounts for a generalized Joule heat source and  $-aT$  describes the coupling to a thermal bath. The definition of the model is completed by the rule that a fuse burns out irreversibly when its temperature reaches the temperature threshold  $T_{th}$  (chosen equal to unity for all fuses). After such a breakdown, we assume that the current distribution in the remaining fuses adjusts itself instantaneously. The dynamics is thus solely controlled by the temperature evolution. Note that after each fuse breakdown, the new calculated set of currents is injected back into the thermal equation (1), with the new initial condition that the temperature of each bond at the beginning of the new heating period is that just reached before the last rupture event. Iterating the procedure again and again after each rupture and denoting by  $t_i$  the time at which the  $i$ th rupture event occurs and  $\{i_n(t_i)\}$  and  $\{T_n(t_i)\}$  the corresponding sets of bond currents and temperatures on all remaining bonds, we obtain the following general time dependent temperature expression for the  $n$ th bond:

$$T_n(t) = T_n(t_i) e^{-a(t-t_i)} + \{G_n^{-1}[i_n(t_i)]^m/a\} \\ \times [1 - \exp\{-a(t-t_i)\}] \\ \text{for } t_i \leq t \leq t_{i+1} \text{ if } T_n(t) \leq 1. \quad (2)$$

### B. Mechanical information

The mechanical analogy is the following:

current	$\Rightarrow$	force
voltage	$\Rightarrow$	vertical displacement
Kirchoff law	$\Rightarrow$	antiplane elasticity
temperature $T$	$\Rightarrow$	damage variable $D$
“Joule” heating	$\Rightarrow$	rate of damage increase under stress
coupling to the heat bath	$\Rightarrow$	work hardening or healing
rupture criterion $T_{th} = 1$	$\Rightarrow$	rupture criterion $D_{th} = 1$

Each bond is now an elastic element, allowed to deform only in the direction perpendicular to the lattice plane, thus defining the so-called antiplane deformation. Then, the tensorial elasticity equation reduces to the Laplace equation for the stress and strain fields (in a homogeneous

system) [10,1(c)]. To make complete the electrical-mechanical analogy, we interpret the temperature as the damage variable characterizing a given element of the lattice. We assume that the damage  $D_n$  of element  $n$  obeys the following equation, which constitutes an exact

translation of Eq. (1):

$$dD_n/dt = G_n^{-1} s_n^m - aD_n. \quad (3)$$

$dD_n/dt$  is the rate of damage process assumed to increase as the  $m$ th power of the stress  $s_n$  on the  $n$ th element. The term  $-aD_n$  accounts for a possible hardening or healing process. This formulation is very similar to the one introduced by Kachanov [11] to describe the propagation of cracks under condition of creep. We also note the analogy with the theory of damage [12]. The rupture criterion is  $D=1$ , i.e., when the damage has reached this threshold, the element is not able to carry any force. It is important to stress the difference with an elastoplastic model in which the deformation is divided into an elastic and a plastic component. Here, the deformation is fully elastic and the damage field does not enter the compatibility condition for the total deformation which is automatically verified by the elastic antiplane deformation. In Refs. [1(b), 1(c)], the term "plastic" was thus misused and should be understood as damage in the sense defined here.

### C. General properties

The simplicity of the model stems from the separation of the time evolution of the electrical (elastic) and thermal (damage) fields: the electric intensity (force) distribution evolves instantaneously under the thermal (damage) rupture of a new bond and the thermal (damage) field changes continuously under the fixed electric current (force) distribution until the next rupture occurs. This feature simplifies the analysis and the numerical computations greatly. Therefore this model is maybe the simplest one can think of which incorporates naturally a dynamics in a statistical model of rupture.

The dynamics present in this model possesses two levels of memory effect. The first level comes through the irreversible evolution of the electric network, similarly to previously studied random fuse models [2]. The second level stems from the memory contained in the additional temperature field which is an additive function of all the previous thermal history of each bond in the network. Moreover, the thermal coupling between each fuse and a bath allows the temperature of each fuse to evolve towards a steady-state value with a characteristic relaxation time.

In order to characterize and classify the properties of the thermal fuse model, we need first to distinguish between the following different situations.

(1) One can choose to impose a constant voltage drop per unit length ( $V$ ) across the system. In this regime, two subcases must then be discussed.

(i)  $V$  is smaller than the threshold  $V_{th}$  ( $=1$  in the units where the conductances  $G$  and the parameter  $a$  are equal to 1 for an infinite uniform network) determined from Eq. (1) by the condition that fuses infinitely far from all boundaries and all cracks reach the temperature rupture threshold  $T_{th}=1$ . In this regime at fixed voltage  $V$ , cracks can grow only when sufficiently large initially so that the current enhancement at their tip is sufficiently large to make them reach eventually the temperature

rupture threshold. In the same regime for a given initial crack, there is a lower voltage threshold (dependent upon the initial shape of the crack) below which the system is stable, and apart from a possible transient, does not suffer any breaking events. Above this lower threshold and below  $V_{th}$ , a rather general solution is the steady-state propagation (at constant velocity) of a crack front. The steady-state nature of the solution is due to the fact that, as the crack length increases, the total conductance decreases. As the voltage is fixed, the input current decreases. Hence there is a competition between the growing current enhancement at the increasing crack tip and the decrease of the bias current. The net effect turns out to be a saturation of the current at the crack tip, making possible the steady-state crack front propagation. We will study this regime in detail in Sec. IV, in relation to the propagation of crack fronts in strips of finite widths.

(ii)  $V$  is larger than the threshold  $V_{th}$ , defined above. Then, in the absence of any crack tip enhancement effect, fuses far from the crack eventually break down in a finite time. It is thus not possible to find steady-state rupture front propagations with a constant velocity. If the system is prepared with some defect or notch, the crack will nucleate from this defect and accelerate without bound [we do not account for the finite electromagnetic (electric case) or acoustic (mechanical case) wave velocity], with an acceleration law which depends on the damage exponent  $m$ . Notwithstanding the fact that all bonds can break in principle, this does not occur in general and the rupture occurs on a small subset as a result of the current amplification at the tip of the growing crack. We have carried simulations in this regime in connection to the question of the determination of the rupture front shape propagating in a strip of finite width (see Sec. V).

(2) One can choose to impose a constant current density ( $I$ ) within the system. For a given initial crack, there exists a current threshold above which the situation is similar to case [(1)(ii)] above. Below this threshold, the system is metastable and does not rupture macroscopically, after a possible transient. Alternatively, imposing a given current, whatever its smallness, there is a minimum crack size (or configuration) above which the crack becomes unstable and accelerates without bound: due to the current enhancement at the crack tip which grows without bound as  $I\sqrt{L}$  in an infinite system, where  $L$  is the crack length, the current at the tip will become larger, for sufficiently large  $L$ , than the threshold to reach the temperature rupture threshold. Below this size, the system is again metastable. Therefore, for a constant applied current, only the accelerated crack regime is found. This case has been addressed already in Refs. [1(b), 1(c)] for a large set of values of  $m$  in disordered network and in Ref. [9] for the special case  $m=1$  with  $a=0$  in homogeneous systems. We come back to this regime in Sec. III for the case of *homogeneous* square lattices with a single small initial nucleating crack.

### III. CATASTROPHIC CRACK GROWTH FROM A NUCLEUS AT CONSTANT APPLIED STRESS

Consider a large square network of size  $L$  by  $L$  as defined in Sec. II, which contains an initial defect at its

center corresponding to the removal of a single bond. At time  $t=0$ , a constant macroscopic current  $I$  is applied to the network. We want to study the geometry of the crack patterns as a function of the applied current and damage exponent  $m$ .

#### A. Nucleation regime in quenched random systems

This problem is suggested from our previous study of quenched random systems in the limit of an applied current  $I$  just above threshold  $I_c$  [1]. Indeed, for a given bond resistance distribution, there exists a minimum value  $I_c$  of the input current necessary for global rupture to occur. Below  $I_c$ , some bond breakdown may occur but the rupture eventually stops before disconnection of the system into two pieces. For  $I$  very close to but larger than  $I_c$ , the rupture process can be decomposed into two steps. The first step is the breaking of the weakest bond, which will then act as a nucleation center. The second step is the growth of a large crack developing from this nucleation center. In the first regime, the Joule heating breaks down the bond which presents the strongest heating power. Once this “hottest” bond is broken, the defect strongly distorts the electric current field around it. Namely, the intensity in the neighboring bonds is typically  $(4/\pi)I$  for the square lattice tilted at  $45^\circ$  with respect to the bus bars. These bonds are thus heated much more efficiently than all the others in the network for small or no disorder. They reach the rupture threshold  $T_{th}$  first. The process goes on with the *connected* growth of a large crack until the final blowup of the total network. We have called this regime the “nucleation” regime [1], since once a bond breaking has been initiated, the evolving rupture grows from this “nucleation” center. This “nucleation” regime occurs only for sufficiently small disorder, so that the Joule heating power  $\approx [(4/\pi)i]^m$  in the bonds at the tip of the first broken bond is significantly larger than all the other heating powers in the other bonds. The first broken bond is always the same, whatever the applied current. However, in the vicinity of the threshold  $I_c$ , slightly different values of the applied current may lead to different breaking patterns, either at the local or global scale, due to the successive ruptures at different positions [1].

The “nucleation” regime is characterized by the growth of a few branches with a degree of sidebranching depending mainly on the damage exponent  $m$ . It is possible to nucleate artificially a similar structure by putting by hand a central crack in a quenched random lattice. Figure 1 presents the resulting rupture patterns obtained with  $m=2$  for different increasing applied currents  $I$  in large systems  $L=180$  with a small disorder on the conductances of the bonds of the lattice, defined by the probability distribution  $P_G(G)$ , chosen uniform in the interval  $[1-\Delta\sigma/2, 1+\Delta\sigma/2]$  with  $\Delta\sigma=0.2$  in this example. For all applied currents, we observe a similar branched structure growing from the nucleus. We note the existence of a diffuse set of small cracks, the more so the larger the applied current. This is the signature of the delay effect contained in Eq. (1) according to which some bonds may finally end up breaking because the accumula-

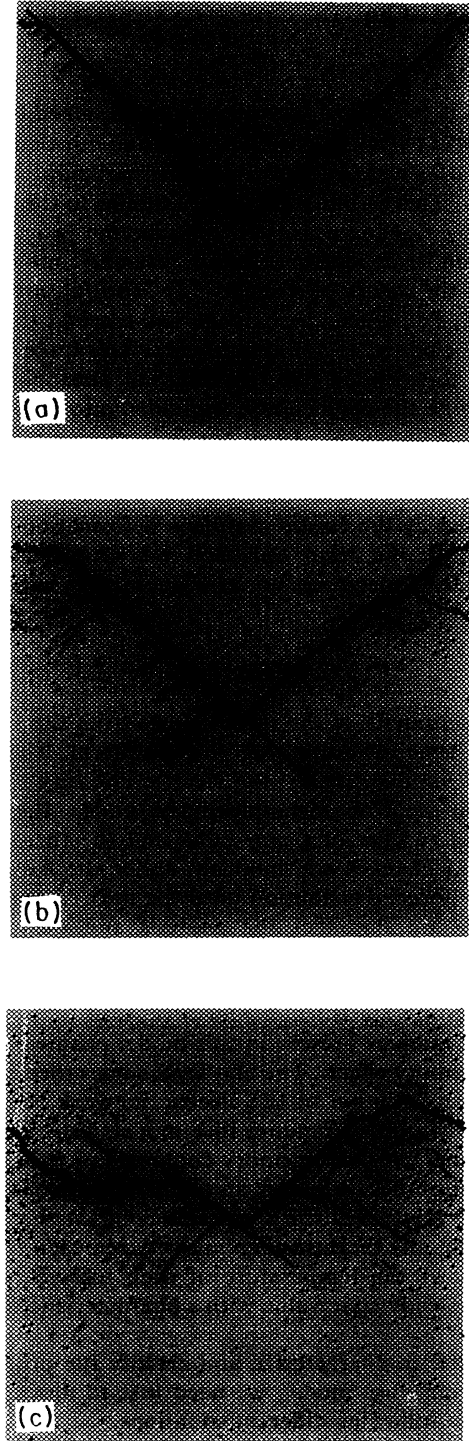


FIG. 1. Typical crack patterns at the final stage of rupture in a square lattice of size 180 by 180 tilted at  $45^\circ$ . The conductances are uniformly sampled in the interval  $[0.9, 1.1]$ . The three pictures correspond to exactly the same disorder realization with, however, different applied currents. (a) Regime close to the rupture threshold:  $I \approx I_c = 0.913$ ; (b) intermediate regime  $I = 1$ ; (c) asymptotic regime  $I = 30$  ( $\gg I_c$ ).

tion of thermal energy allows them to reach the rupture threshold, even if their heating rate is not very large. When increasing the applied current from  $I=I_c$  to  $+\infty$ , we thus observe a crossover from a regime characterized by a sidebranching, reminiscent of dendritic growth, to a regime where the sidebranching as well as the main crack become very disordered. This stems from the fact that the effect of the quenched disorder on the rupture growth is less important for small  $I$ , dominated by current amplification at the crack tips, than for large  $I$ 's dominated by disorder. The three figures 1(a)–1(c) should be compared to Figs. 7(a)–7(c) presented in Ref. [1(b)] under the same conditions except that the central defect was absent in Ref. [1(b)]. The straight crack structures are absent in this case for intermediate and large current since the main mechanism becomes that of damage dominated by the disorder, and not the nucleation and growth of a single branched crack.

### B. Crack growth from a central nucleus in ordered systems

In order to pinpoint the origin of the branching process observed above and in [1(b)], we were thus led to study the growth of a crack in a *perfectly ordered* lattice possessing a central nucleus of unit mesh size, in a way similar to a small notch in standard mechanical tests. Much to our surprise, we found an extremely rich phenomenology of shapes (four-leafed clover, fingers, dendritic-like side bifurcation, needles) as the creep exponent is changed from 0 to  $+\infty$ , as shown in Figs. 2 and 3. This interesting regime is observed for a total applied current much larger than the threshold  $I_c = \pi/4 = 0.785$ . For these large applied currents, we have previously shown [1(b)] that the sequence of rupture and crack patterns becomes independent of  $I$  (this is the regime where the coupling with the heat bath is negligible in comparison to the Joule heating term). In this case, for  $m \geq 1$ , the growing cracks are structures oriented at  $45^\circ$  with respect to the horizontal bus bars. For smaller  $m$ , the cracks are more complex structures, which tend to take the geometry of the infinite cluster at the percolation threshold, as  $m \rightarrow 0$  [1]. On the contrary, the regime just above threshold is characterized by the strongest sensitivity with respect to perturbations [1] due to the competition between the Joule heating and the coupling with the thermal bath.

Figure 2 shows the set of elements which have broken at increasing times during the rupture process for three different values of the damage exponent  $m$ : (a)  $m=0.02$ , (b)  $m=0.8$ , and (c)  $m=2.2$ . The chosen times are such that the size of the patterns is much smaller than the lattice size ( $\leq 0.2L$  at most), ensuring small corrections due to finite size effects which are known to be extremely important for large cracks (see [13], and references therein). For all values of  $m$  which have been studied, the patterns appear to be growing in a self-similar way, with a size rescaling allowing deduction of the pattern at a given time from that at a previous time. The set of ruptured elements presents a shape which remains constant as a function of time (homothetic) and the dynamics of growth of the crack is described by the knowledge of a single scaling factor giving the size  $r(t)$  of the crack. As stated

above, at longer times, finite size effects become important and distort the shape with a breakdown of self-similarity in time. For the early times, it is thus possible to attribute to each  $m$  a well-defined crack topology. The dependence of this crack topology on the damage exponent  $m$  is given in Fig. 3. For small  $m$ , cracks present the shape of a four-leaf clover with an orientation breaking the  $\pm 45^\circ$  symmetry of the underlying lattice, due to the initial orientation of the crack nucleus. When increasing the exponent  $m$ , the cracks keep the characteristic four-leaf clover shape. However, their orientation is modified and they rotate counterclockwise as  $m$  increases. Furthermore, the central ruptured zone, containing broken elements in the two  $\pm 45^\circ$  directions, shrinks and eventually disappears around  $m=0.3$ . For this value and above, the cracks have their four branches now perfectly oriented at  $\pm 45^\circ$ . The branches shrink in width as  $m$  increases. Figure 2(b) shows the shape of the growing crack for  $m=0.8$ . We observe again a self-similar regime in time at small times such that the finite size effect is not felt. At longer times, the fingers thicken. Note that in this regime, the crack grows by accreting new rows of broken elements growing from the initial nucleating central crack. When  $m$  tends to 1, we have observed an extremely intriguing set of transitions, characterized first at  $m=0.98$  by the fusion between the two up and the two bottom fingers. Around  $m=0.99$ , sidebranching occurs in the form of two thick branches growing from the side in the middle part of two opposite main branches. At  $m=0.995$ , further sidebranching occurs and seems to proliferate. At  $m=1$  exactly, a single sidebranching, one for each branch is recovered which is characterized by a smooth envelope starting from the tips of the main branches. As  $m$  increases further, these sidebranches rupture into sub-branches. The patterns in Fig. 2(c) illustrate the typical shapes of the cracks for  $m$  significantly larger than 1 (here  $m=2.2$ ) at increasing times. Again, we observe the self-similarity in time, by comparing the shapes at the three increasing times. The sidebranching, which is present for  $m$  up to approximately 2.5, disappears for larger values, where only two straight branches dominate.

The existence of thick fingerlike patterns for low  $m$  is reminiscent of finger patterns obtained, for instance, in the Saffman-Taylor problem of a low density fluid pushing a larger density fluid in a channel [6,7]. The sidebranching phenomena observed for  $m$  around 2 and above are very similar to those characterizing the growth of dendrites in solidification problems [6,7]. Particularly intriguing in an ordered deterministic system is the observation of an irregular system of secondary branches in this regime ( $m \geq 2$ ). These structures are the geometrical consequence of the large sensitivity of the growth phenomenon with respect to disturbances. In our numerical simulations, there exists a residual numerical noise, which when amplified by the nonlinear dynamics is the cause of the chaotic sidebranches. This is verified by adding a controlled annealed noise to the current field or to the temperature field which results in much enhanced disorder in the sidebranching patterns. The existence of a small quenched disorder on the conductances (see Fig.

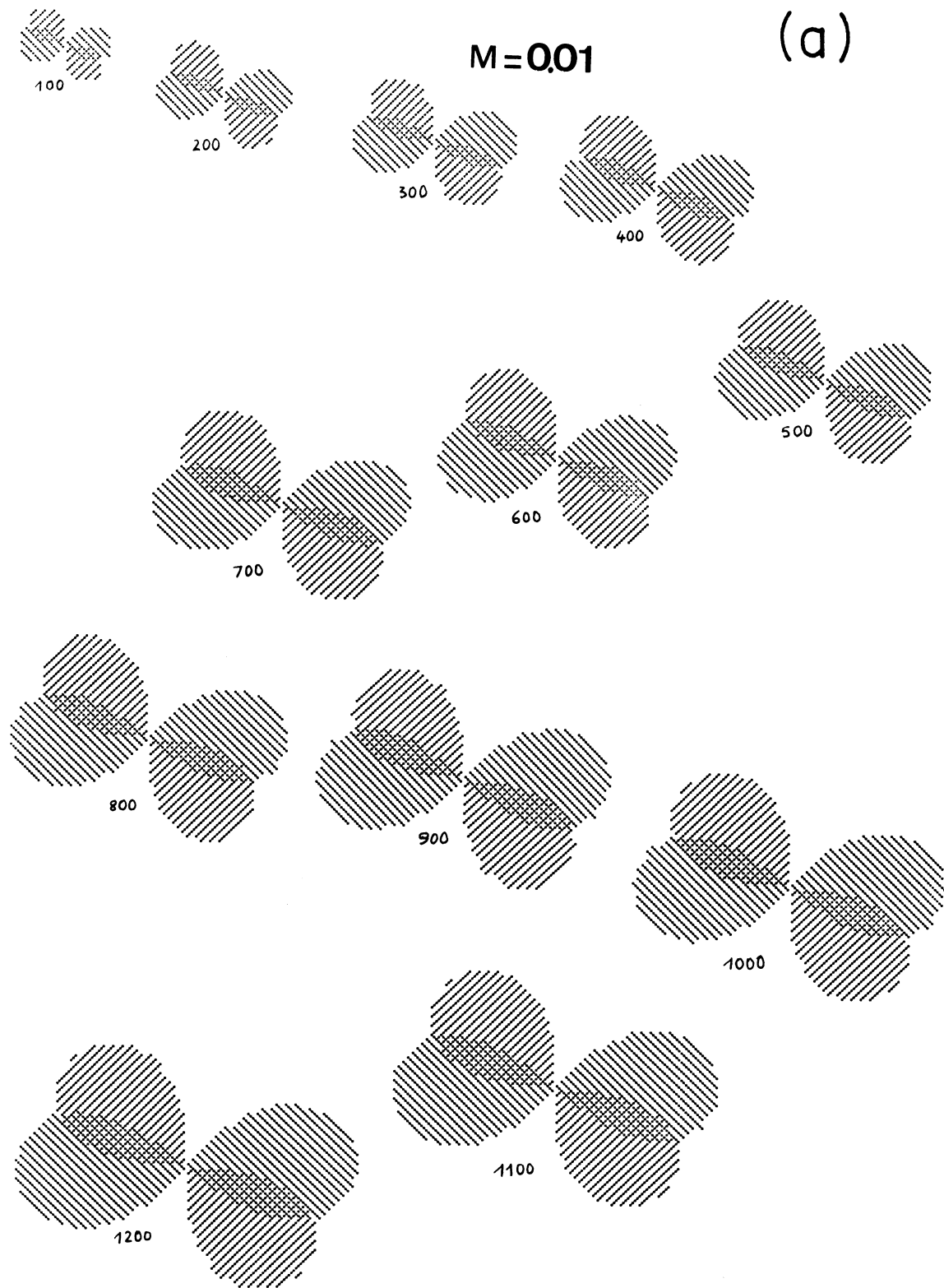


FIG. 2. Snapshots at increasing times of the set of ruptured elements for a constant applied current  $I=30$ . Since the crack borders are accelerating in an explosive way, we represent the crack patterns at increasing numbers of ruptured bonds (indicated below each corresponding crack pattern). (a)  $m=0.01$ : note the four-leaf-cloverlike shape which grows in a self-similar way up to a size where distortion occurs due to finite lattice size effects; (b)  $m=0.8$ ; (c)  $m=2.2$ : this shape is typical for values of  $m$  larger than 1 (for  $m$  larger than 4 typically the sidebranching disappears).

1) also results in more irregular sidebranches. Sidebranching can thus be attributed to an amplification at scales of the mesh size of noisy fluctuations on the side of the advancing cracks. This noise amplification relies on

the conjunction of the threshold nature of rupture, the long-range electric interaction, and the delay effects induced by the temperature field. This is in contrast to the mechanism of sidebranching which has been proposed in

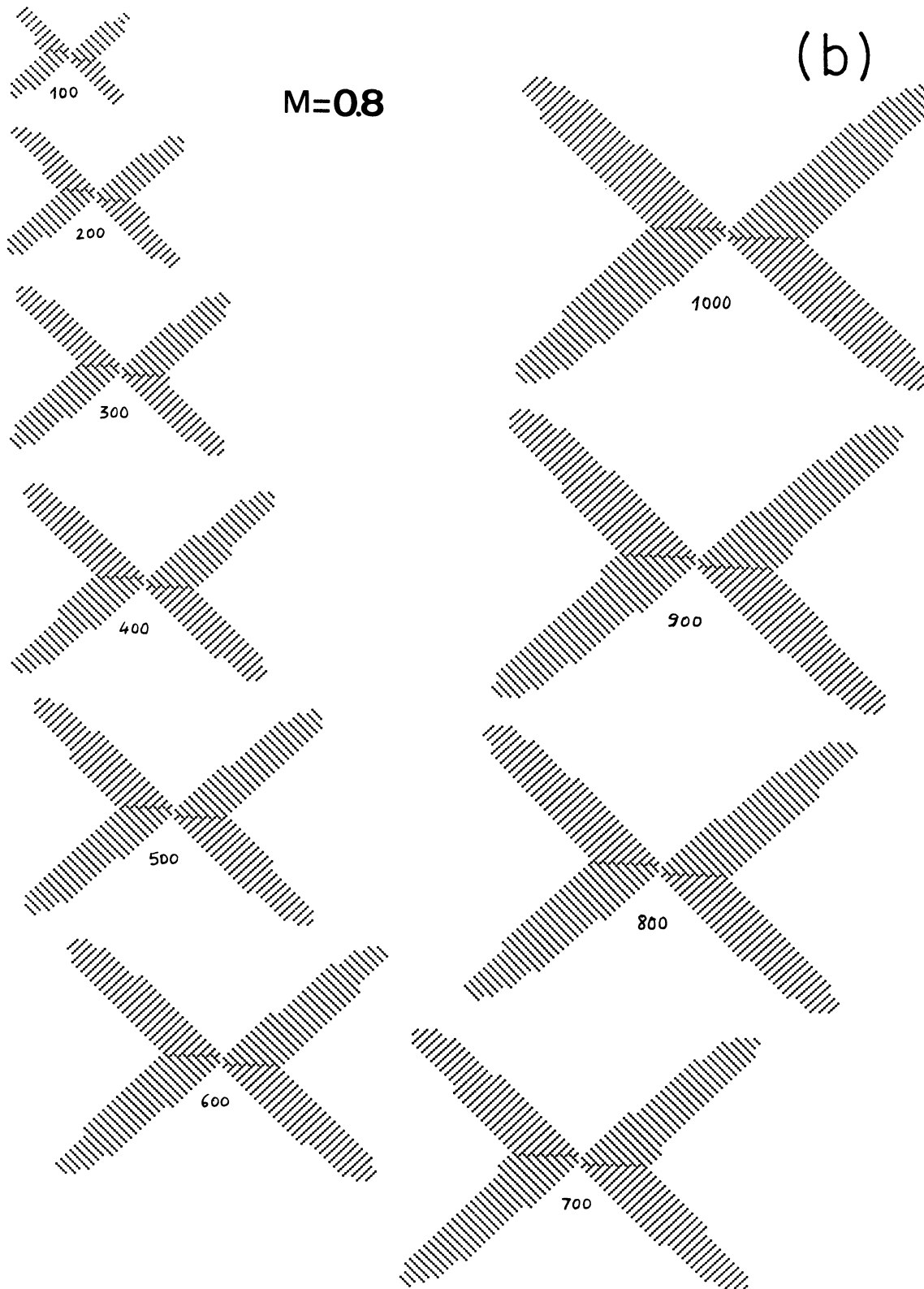


FIG. 2. (Continued).

dendritic solidification [14] relying on a wavelength selective amplification of noise near the tip which is then convected behind.

#### IV. STEADY-STATE CRACK GROWTH IN STRIPS UNDER CONSTANT APPLIED DISPLACEMENTS

The observation of dendriticlike crack patterns in Figs. 2 and 3 suggests further exploration of a possible analogy

between the formation and propagation of a crack in our thermal fuse model and the propagation of fronts in solidification or viscous fingering problems [6,7]. The work of Barber, Donley, and Langer [15] has also addressed this question of a possible analogy between the propagation of cracks in strips and that of solidification fronts or of viscous fingers in channels. They studied the problem of velocity selection in the propagation of a

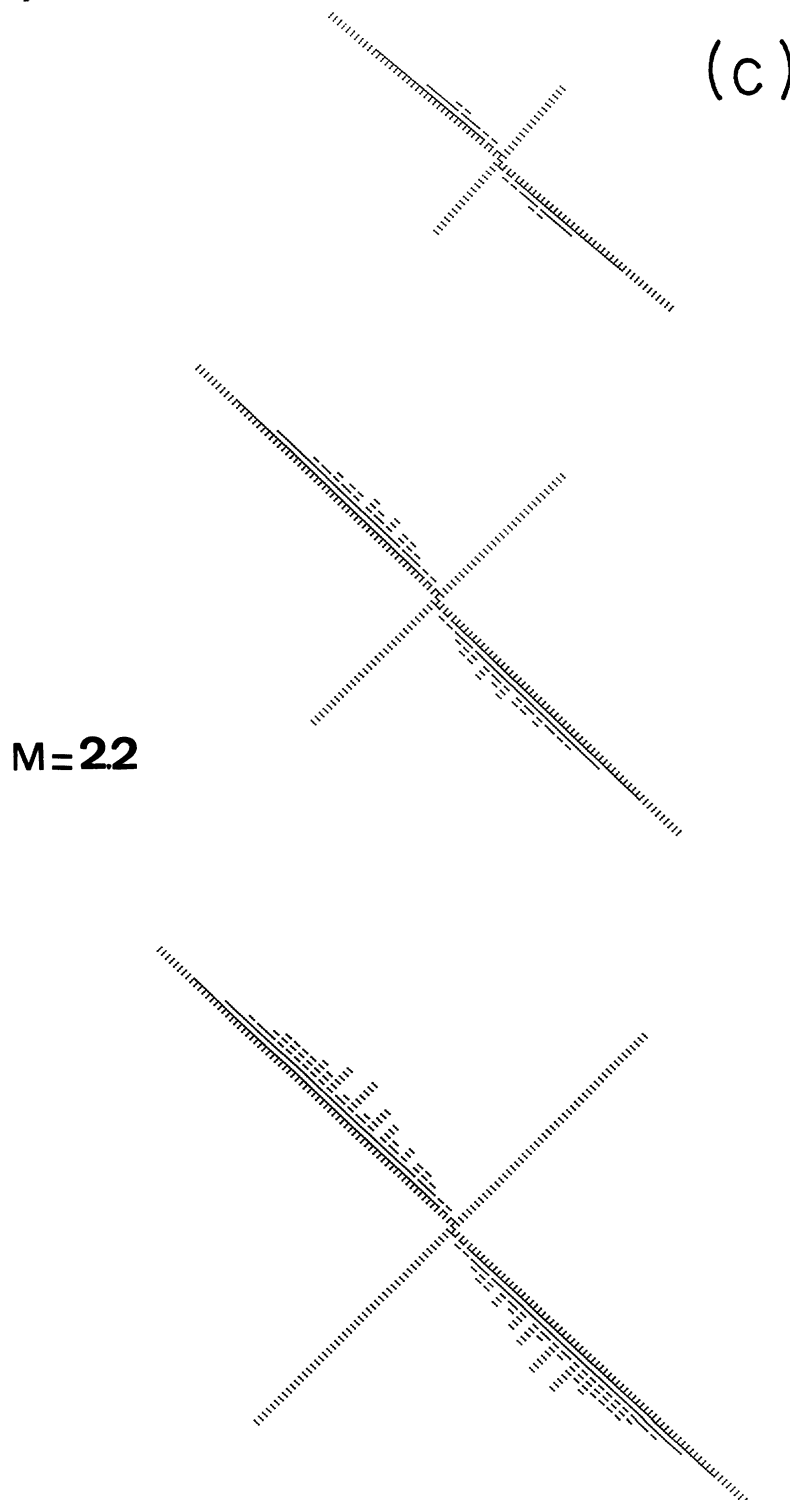


FIG. 2. (Continued).

crack in a viscoelastic medium, showing memory effects. Contrary to solidification fronts or viscous fingers whose velocity is determined by a microscopic characteristic scale, the capillary length when surface tension is present [16], there are no analogous subtleties in the crack propagation problem. It was found in Ref. [15] that the crack

tip velocity is unique and simply selected by a balance between mechanical work and viscous dissipation. We address the same question of the shape and velocity selection of cracks in the context of the thermal fuse model and find a result similar to the Saffman-Taylor problem, i.e., a continuum of crack solutions parametrized by the

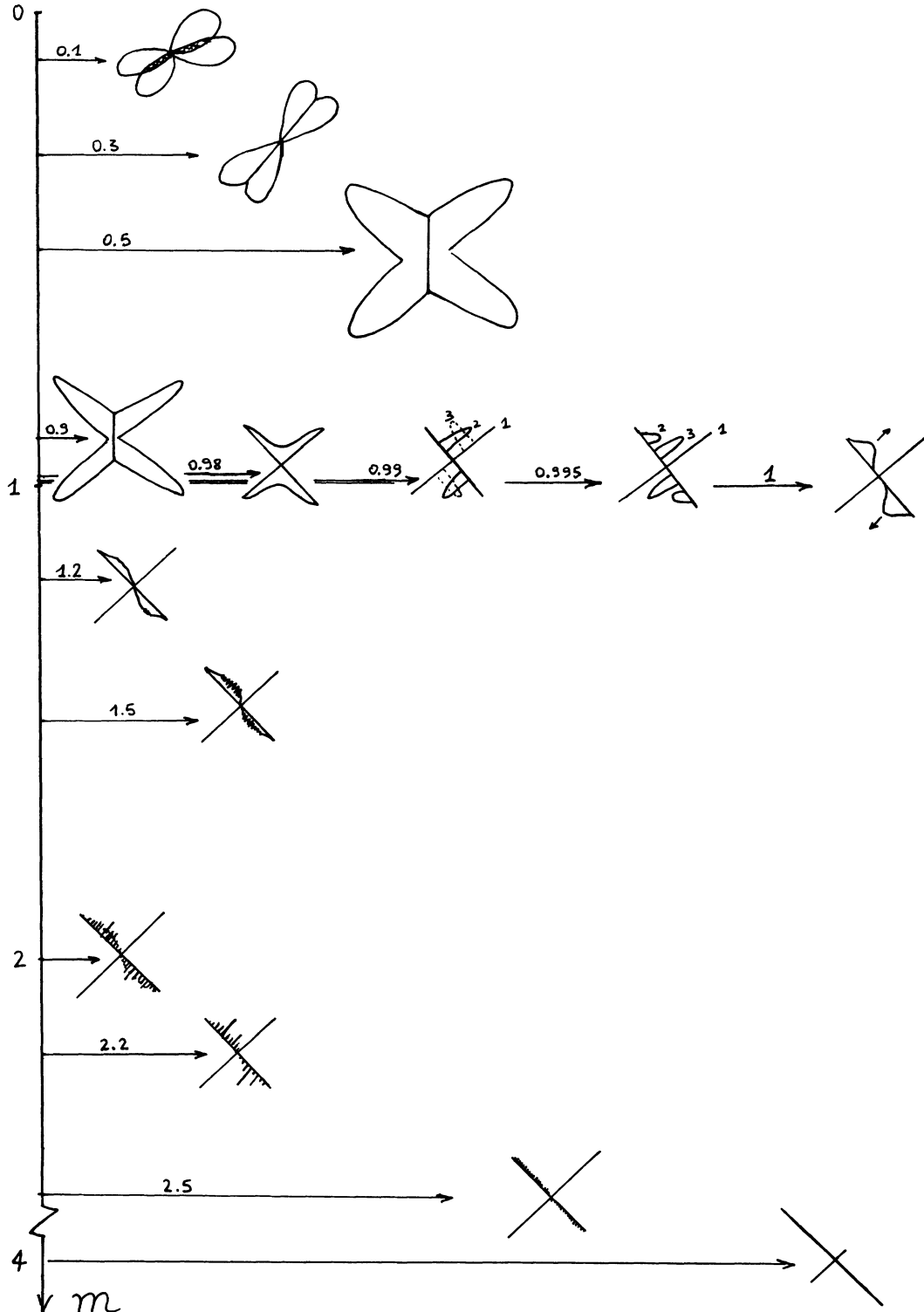


FIG. 3. Schematic "phase diagram" showing the dependence of the crack topology on the damage exponent  $m$  in the case where a crack grows from a central nucleus under constant applied stress.

velocity. The difference with the work of Barber, Donley, and Langer [15] stems from the different physical ingredients: in our case, rupture does not obey an energy balance but is controlled by the damage variable (temperature in the electrical fuse language) which involves a long time accumulation over history.

#### A. Analytic calculation in a narrow strip with a central semi-infinite crack

Consider a strip of width equal to three meshes of a nontilted square lattice. The upper boundary is put at constant voltage  $V$  and the lower one at voltage 0. Consider the existence of a semi-infinite crack extending from  $-\infty$  to bond 0 as shown in Fig. 4. We are looking for a solution in which the crack tip propagates at a constant velocity  $U$ , if it exists. We now exploit the simplicity of the thermal fuse model, appearing in the decoupling between the electric field and the thermal field controlling the rupture. Since we are looking for a solution for a crack moving at a constant velocity, it is then enough to solve for the current field in the semi-infinite crack geometry and to move this solution in the frame of the advancing crack. Knowing the current on all bonds, we will then plug it into the thermal equation (1) in order to find the velocity  $U$ . The analysis will show that this solution is stable against branching or velocity fluctuations.

Due to the symmetry of the problem, we need only to determine the voltages  $W_0, W_1, \dots, W_n, \dots$  at nodes  $0, 1, \dots, n, \dots$  to  $+\infty$  and the voltages  $V_1, V_2, \dots, V_n, \dots$  at the nodes  $-1, -2, \dots, -n, \dots, -\infty$  in the lines shown in Fig. 4. The Laplace equation yields (see Fig. 5)

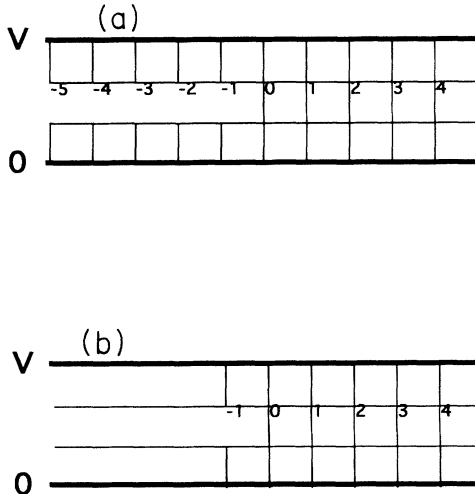


FIG. 4. Geometry of the strip of width equal to three meshes of a nontilted square lattice. The upper boundary is put at constant voltage  $V$  and the lower one at voltage 0. (a) Case of a semi-infinite crack extending from  $-\infty$  to bond 0 and placed on the central row; (b) semi-infinite crack of total asymptotic thickness equal to the whole strip width, with one mesh difference between the first and second row and the central one.

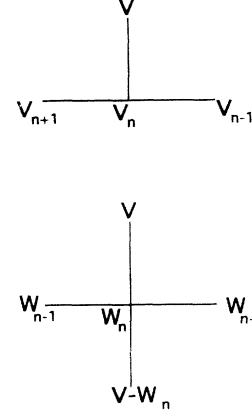


FIG. 5. Definition of the voltages  $W_0, W_1, \dots, W_n, \dots$  at nodes  $0, 1, \dots, n, \dots$  to  $+\infty$  and the voltages  $V_1, V_2, \dots, V_n, \dots$  at the nodes  $-1, -2, \dots, n, \dots, -\infty$  which allow us to derive the recurrence equation from the Laplace equation.

$$V_{n+1} + V_{n-1} - 3V_n + V = 0, \quad (4a)$$

$$W_{n+1} + W_{n-1} - 5W_n + 2V = 0, \quad (4b)$$

whose physical nondiverging solutions are, respectively,

$$V_n = V - Cs_3^{n+1}, \quad (5a)$$

$$W_n = 2V/3 + C's_5^n, \quad (5b)$$

where

$$s_3 = (3 - \sqrt{5})/2 \approx 0.382, \quad (6a)$$

$$s_5 = (5 - \sqrt{21})/2 \approx 0.209. \quad (6b)$$

The two constants of integration  $C$  and  $C'$  are determined from the two matching conditions on the nodes  $-1$  and  $0$ :

$$W_0 + V_2 + V - 3V_1 = 0 \quad (\text{node } -1), \quad (7a)$$

$$W_1 + V_1 + 2V - 5W_0 = 0 \quad (\text{node } 0). \quad (7b)$$

This yields

$$C = (V/3)(4 - s_5)/[(3 - s_3)(5 - s_5) - 1], \quad (8a)$$

$$C' = (V/3)c,$$

$$\text{where } c = (2 - s_3)/[(3 - s_3)(5 - s_5) - 1]. \quad (8b)$$

The current flowing in the  $n$ th central vertical bond is then

$$\begin{aligned} i_n &= W_n - (V - W_n) \\ &= 2W_n - V \\ &= V/3 + 2C's_5^n = (V/3)[1 + 2cs_5^n], \end{aligned} \quad (9)$$

considering that all bonds have the same unit conductance. The constant  $c$  has been defined in Eq. (8b).

Let us now use this result to determine the thermal history of the fuses in front of the propagating crack and its velocity. Since we are looking for a constant velocity  $U$  of the crack, the time interval  $\Delta t$  during two successive breaking events is constant:

$$\Delta t \equiv U^{-1}, \quad (10)$$

taking a unit square lattice mesh. In the frame moving with the crack tip at constant velocity  $U$ , the temperature profile on the bonds in front of the crack is stationary, as is the current distribution which allows the use of the static solution (9). Let us call  $\theta_0, \theta_1, \dots, \theta_n, \dots$  the temperature of the bonds  $0, 1, \dots, n, \dots$  just after the breaking of bond  $-1$  (corresponding to the progression of the crack by one unit lattice mesh) and take the time of this event as the origin of time. Using Eq. (2) for all bonds with  $G_n = 1$  for all  $n$  yields

$$T_0(t) = \theta_0 e^{-at} + (i_0^m/a)[1 - e^{-at}], \quad (11a)$$

$$T_1(t) = \theta_1 e^{-at} + (i_1^m/a)[1 - e^{-at}], \quad (11b)$$

⋮

$$T_n(t) = \theta_n e^{-at} + (i_n^m/a)[1 - e^{-at}]$$

⋮

$$\text{for } n \text{ up to } +\infty, \quad (11c)$$

where  $i_n$  is given by Eq. (9). The next rupture event will take place on bond 0 which first reaches the rupture criterion  $T_0(t = \Delta t) = T_{th}$  at time  $t = \Delta t$ . At this time, for a crack propagation at a constant velocity,  $T_1(t = \Delta t) = \theta_0, \dots, T_n(t = \Delta t) = \theta_{n-1}, \dots$ , for  $n$  up to  $+\infty$ . Eliminating the  $\theta_n$ 's yields the following equation for  $\Delta t$ :

$$T_{th} = a^{-1} [1 - e^{-a\Delta t}] \{ i_0^m + i_1^m e^{-a\Delta t} + i_2^m e^{-2a\Delta t} + \dots + i_n^m e^{-na\Delta t} + \dots \}. \quad (12)$$

Inserting Eq. (9) into Eq. (12) determines  $\Delta t$  as a function of  $V$  and  $a$ . Let us restrict our attention to the simple case  $m = 1$  which yields  $T_{th}$  in Eq. (12) under the form of a simple geometric series. It then gives easily

$$\Delta t = a^{-1} \ln \left\{ \frac{s_5 \left[ \frac{3aT_r}{V} - 1 \right] - 2c}{\frac{3aT_r}{V} - 1 - 2c} \right\}, \quad (13)$$

where  $c$  has been defined in Eq. (8b). Using the values of  $s_3 = 0.3820$ ,  $s_5 = 0.2087$ , and  $c = 0.1402$  [Eqs. (6) and (8b)], expression (13) can then be cast into the form

$$e^{-a\Delta t} = 5[X - 1.28]/[X - 2.33], \quad (14)$$

where

$$X = 3aT_{th}/V. \quad (15)$$

Since we are looking for positive  $\Delta t$ 's,  $e^{-a\Delta t}$  takes values in the interval  $[0, 1]$ . From Eq. (14), this constrains the

possible values of  $X$  in the interval  $1.01 \leq X \leq 1.28$ . We find that  $\Delta t \rightarrow 0$ , i.e.,  $U \rightarrow +\infty$  as  $X \rightarrow 1.01$  whereas  $\Delta t \rightarrow +\infty$ , i.e.,  $U \rightarrow 0$  as  $X \rightarrow 1.28$ . In between, the crack velocity crosses over continuously from  $+\infty$  to 0. The velocity  $U$  of the crack tip as a function of the parameter  $X$  is shown in Fig. 6. These two limiting behaviors have simple interpretations. For  $X \rightarrow 1.01$ , the applied voltage drop is high and is such that the bonds far away from the tip are close to rupture even in the absence of the current enhancement effect produced by the presence of the crack tip. It is then natural to expect a diverging velocity if all bonds can rupture almost simultaneously, even far away from the crack. In the other limit  $X \rightarrow 1.28$ , the applied voltage drop is small and is such that the highest current  $i_0$  in the network is barely large enough to heat the fuse placed at the crack tip up to the temperature threshold  $T_{th} = 1$  even in an infinite time. It is thus natural to expect a vanishing velocity in this case. For  $X > 1.28$ , i.e., for a small applied voltage  $V$ , the crack does not propagate since no bond can reach the temperature threshold. For  $X < 1.01$ , bonds far away from the crack tip blow up simultaneously in the network. It is not possible to obtain a crack propagation at constant velocity in this regime since the whole network is unstable. We will show below that, in this regime of large applied voltages, it is possible to obtain connected cracks growing in an accelerated way from a nucleus.

This discussion is valid as long as the parameter  $a$  quantifying the coupling with the thermal bath (or the hardening process in the mechanical analog model) is not vanishing. Indeed, for  $a = 0$ , there is no solution to the problem since any nonvanishing current always leads to an unbounded heating of the bonds. The bonds far away from the tip have always enough time to reach the rupture threshold and do it independently of the crack tip propagation. This case is thus similar to the one for  $a \neq 0$  with  $X < 1.01$  in which there are no solutions with a crack growing at a constant velocity. The above results have been derived analytically for  $m = 1$ , which is the simplest case. Similar qualitative behaviors hold as long as  $m > 0$ , with of course different intervals on the applied voltage drop in which a solution exists. The case  $m \rightarrow +\infty$  is also easy to analyze and shows that the crack

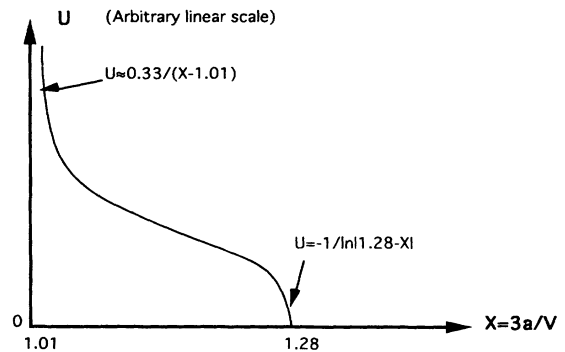


FIG. 6. Velocity  $U$  of the crack tip as a function of the parameter  $X = 3aT_{th}/V$  for  $m = 1$  in the geometry defined in Fig. 4(a).

tip velocity is a monotonous increasing function of  $m$  at fixed  $V$ . This trend can also be checked to hold for all positive values of  $m$ , at fixed  $V$ .

We have considered the case where the semi-infinite crack is just in the middle of the strip. It is also interesting to examine the case of other crack shapes, such as, for instance, the one shown in Fig. 4(b), and ask the question of whether such a shape can propagate undeformed. In the moving frame, it is easy to solve for the node potential and current distribution, in a way similar to what has been done previously. The condition that the first and third rows propagate at the constant velocity  $U=1/\Delta t$  provides a first equation for  $\Delta t$ , which for  $m=1$  reads

$$1 = \frac{V}{3a} (1 - e^{-a\Delta t}) \left\{ \frac{4 - s_5}{9 - 2s_5} + \frac{e^{-a\Delta t}}{1 - e^{-a\Delta t}} - \frac{\tilde{c}s_5 e^{-a\Delta t}}{1 - s_5 e^{-a\Delta t}} \right\},$$

where  $\tilde{c} = \frac{1}{s_5(9 - 2s_5)}$ .

The condition that the central row propagates at the same constant velocity  $U=1/\Delta t$  gives a second equation for  $\Delta t$ , which for  $m=1$  reads

$$(1 - e^{-a\Delta t}) = \frac{\left(1 - \frac{V}{3a}\right)(1 - s_5)}{2\tilde{c}_5}.$$

These two equations are in general incompatible except for certain values of the couple  $(V, a)$ . For a discrete set of such values, in addition to having the single row solutions, many other shapes, deduced from generalizations of the shape represented in Fig. 4(b), can propagate in an undeformed way. Note that the degeneracy for  $\Delta t$  of the two above equations occurring for certain values of  $(V, a)$  can be interpreted as a ‘‘commensurability’’ criterion stemming from the discrete nature of the network, such that the time intervals between successive bond ruptures are equal for different rows. The case of a semi-infinite crack in one of the lines of vertical bonds in contact to one of the bus bars can be studied in a similar way. We also find a solution with a constant velocity with, however, a smaller velocity than for the central crack shown in Fig. 4(a) and a different voltage interval in which the solution exists. A similar analysis can be carried out for strips of larger finite widths  $L$  [17] and for the  $L$  possible positions of the semi-infinite crack as well as for other more complex shapes. The analysis becomes, however, more cumbersome as  $L$  increases. Again, for the same applied voltage, the semi-infinite crack at the center possesses the largest velocity, since this configuration produces the largest current enhancement effect at the crack tip. As the channel width increases, the geometry of the crack becomes more sensitive to any quenched disorder that it may encounter in its growth, due to the diminishing lateral confinement of the bus bars. It may thus begin to meander laterally with respect to its main growth direction, as found in square systems in the presence of a large disorder.

The main conclusion of this work is the finding that, for a given geometry, the crack tip velocity is uniquely

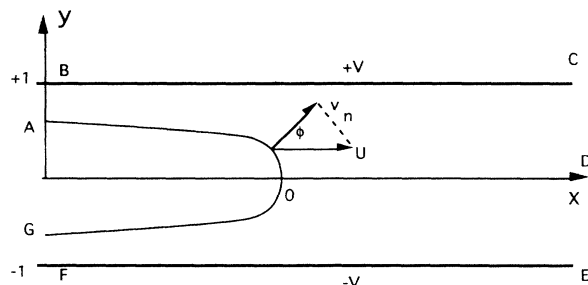


FIG. 7. Strip geometry showing the crack having the shape of a finger and propagating in an undeformed way at a constant velocity  $U$ . A constant voltage  $\pm V$  is applied at the two bus bars  $y = \pm 1$ .

determined by a nonlocal growth criterion involving the increase of the temperature (damage field) at all points ahead of the crack tip, as seen from Eq. (12) with (10). The crack tip velocity is solely determined by the time needed to heat a fuse from  $T=0$  at  $x \rightarrow +\infty$  to  $T=1$  on the crack tip. The coexistence of several solutions for the same applied voltage (the finite number coming from the finite width of the strip) suggests that the crack front velocity problem could be similar in the continuous limit to the class of interface growth problems exemplified by the Saffman-Taylor problem which has an infinity of degenerate solutions in the absence of surface tension. However, in our problem, the different solutions are stabilized by the discreteness of the lattice and it is not clear *a priori* what occurs for a continuous system. In the following section, we examine this question.

## B. Continuous formulation

In order to pinpoint further the common aspects and the differences, if any, between the present thermal fuse model and more general growth phenomena, we present the continuous formulation of the previous problem of a semi-infinite crack front propagation in a strip of finite width with a constant voltage (displacement) applied to its borders.

Let us consider the geometry shown in Fig. 7 in which the ‘‘crack’’ is the interior domain of the curve  $AOG$ . Note that we allow for a crack geometry which is not a line in 2D but rather a finger of finite width. This is suggested from the numerical simulations presented in Sec. III which showed fingerlike solutions for small  $m$ . In the ruptured interior domain of the curve  $AOG$ , the current is zero. Elsewhere in the strip, the potential at point  $(x, y)$  is denoted  $\Phi(x, y)$ . Let us note  $y = \pm f(x)$ , for  $-\infty < x \leq 0$ , the equation giving the boundary of the ruptured region, taking the origin at the tip of the crack. The continuous version of the thermal fuse model for the steady-state propagation of a cracked front is defined by the following set of equations written in the frame moving with the crack:

$$\nabla^2\Phi=0 \text{ for all points outside the crack (Kirchoff law) ,} \quad (16a)$$

$$\Phi(X,y=\pm 1)=\pm V \text{ (imposed potential on the two bus bars) ,} \quad (16b)$$

$$\partial\Phi/\partial n|_{y=\pm f(x)}=0 \text{ (zero current flowing through the crack boundary) ,} \quad (16c)$$

$$-U\partial T/\partial X=G^{m-1}|\nabla\Phi|^m-aT \text{ (thermal heating and coupling thermal bath) ,} \quad (16d)$$

$$T(X\rightarrow+\infty,y)\rightarrow G^{m-1}(2V/G)^m/a \text{ (uniform asymptotic temperature far ahead of the crack) ,} \quad (16e)$$

$$T(X,y=\pm f(x))=1 \text{ for } -\infty < x \leq 0 \text{ (rupture condition on the crack border) .} \quad (16f)$$

Equation (16d) is the continuous version of Eq. (1) written in the frame moving at the constant velocity  $U$  of the crack. Note that no thermal diffusion is taken into account, in agreement with the definition (1) of the model. The term  $-U\partial T/\partial x$  stems from the change of variables  $(x,y,t)\rightarrow(X=x-Ut,y)$  and corresponds to the time derivative of a solution of the form  $T(x,y,t)=T(x-Ut,y)$  propagating in an underformed way at the constant velocity  $U$ .  $U$  is *a priori* unknown as in Sec. IV A and must be determined from the set of Eqs. (16). In the frame moving at  $U$ , the crack geometry, the electric potential, current density, and the temperature field are constant.  $G$  is the conductivity of the strip defined by  $j(x,y)=G\nabla\Phi$ . Equation (16f) expresses the fact that the boundary of the crack is by definition just at the threshold temperature  $T_{\text{th}}=1$  for rupture.

The problem of the steady-state propagation of a semi-infinite crack front in a strip of infinite width at which border are applied constant displacements appears very similar to the Saffman-Taylor problem of the penetration of a single finger of air into a Hele-Shaw channel of thickness  $b$  and width 2 filled with a fluid of viscosity  $\mu$ . In this case, the equations governing the steady-state propagation of the finger in the frame moving with the finger read

$$\nabla^2\Phi=0 \text{ (mass conservation for an incompressible fluid) ,} \quad (17a)$$

$$\nabla\Phi(x,y=\pm 1)=U \text{ (vanishing fluid velocity on the two borders) ,} \quad (17b)$$

$$\partial\Phi/\partial n|_{y=\pm f(x)}=0 \text{ (zero fluid flux flowing through the finger boundary) ,} \quad (17c)$$

$$\nabla\Phi=-(b^2/12\mu)\nabla p \text{ (Darcy's law) ,} \quad (17d)$$

$$p(x\rightarrow+\infty,y)\rightarrow 0 \text{ (uniform low pressure far ahead of the finger) ,} \quad (17e)$$

$$p(-\infty < x \leq 0, -f(x) \leq y \leq +f(x))=1 \text{ (uniform high air pressure in the finger) .} \quad (17f)$$

$\Phi$  is the velocity potential in water defined by  $\mathbf{v}=\nabla\Phi$ ,  $\mathbf{v}$  is the flow velocity (averaged along the transverse direction to the Hele-Shaw plane), and  $U$  is the velocity of the finger.  $p(x,y)$  is the pressure in water at point  $(x,y)$ . The two problems obey the same Laplace equations (16a) and (17a). The boundary conditions on the two strip borders are dual to each other (imposed  $\Phi$  for the crack problem [Eq. (16b)] and imposed  $\nabla\Phi$  for the air finger problem [Eq. (17b)]). The boundary conditions on the crack and finger boundary are identical [Eqs. (16c) and (17c)]. Equations (16e) and (17e) are essentially identical since they impose a constant value to the additional field (the temperature in the crack case and the pressure in the finger case) very far from the tip of the crack (finger). Equations (16f) and (17f) are identical in the sense that the crack and finger boundary corresponds to the iso-value of the additional field. Equations (16d) and (17d) both allow us to determine the additional field from the potential  $\Phi$ . However, they are quite different since Eq. (17d) is local and in fact yields  $p=-(12\mu/b^2)\Phi+\text{const}$ , showing that, with Eq. (17f), the finger boundary is an equipotential. This implies with Eqs. (17c) and (17d) that the local normal velocity of the air-water interface is proportional to the normal component of the pressure gradient:  $v_n\sim\partial p/\partial n\sim\partial\Phi/\partial n$ . This local growth law is common to many other surface growth phenomena. In contrast, the determination of the temperature field is a

nonlocal problem in the sense that it demands the solution of the partial differential Eq. (16d) with boundary conditions (16e) and (16f). Assuming a crack boundary profile  $y=\pm f(x)$ , one can solve for the potential field  $\Phi$  solution of Eqs. (16a)–(16c). Then, the question is that of the existence of a solution for the temperature field obeying Eqs. (16d) and (16f) with some velocity  $U$ .

It is possible to write an expression similar to  $v_n\sim\partial p/\partial n\sim\partial\Phi/\partial n$  (valid for the Saffman-Taylor problem) for the crack case. Indeed, consider an arbitrary point on the moving crack boundary. Then the velocity of this point is  $v_x=U$  and  $v_y=0$  since its motion is parallel to the  $0x$  axis. The component of this velocity normal to the boundary is given by  $v_n=v_x\cos\phi=U\cos\phi$ , where  $\phi$  is the angle between the normal to the boundary and the  $0x$  axis. Using  $U$  obtained from Eq. (16d) yields the local growth velocity of the crack,

$$v_n=-[G^{m-1}|\nabla\Phi|^m-aT]/(\partial T/\partial n) , \quad (18)$$

where we have replaced  $\cos\phi(\partial T/\partial x)$  by  $\partial T/\partial n$ . This holds because the crack boundary is an isotherm and the gradient of the temperature is thus normal to it.

We now indicate how to solve for the crack shape  $y=\pm f(x)$ . First, we write the formal solution of Eq. (16d) as

$$T(x,y)=-G^{m-1}U^{-1}e^{ax/U}\int_{cte}^x|\nabla\Phi(x',y)|^me^{-ax'/U}dx' , \quad (19)$$

where the constant  $cte$  is determined from the condition (16e). The crack boundary is the loci of points  $(x,y)$  such that  $T(x,y)=1$ , which, using Eq. (19), yields an implicit equation  $y=\pm f(x)$ , once  $\Phi(x,y)$  is known. The difficulty of the problem stems from the fact that the shape  $y=\pm f(x)$  must be made compatible with the electric potential field which must obey Eqs. (16a)–(16c). We explain in Appendix A the general method for solving the problem.

There is a degenerate case for which the analysis can be carried out explicitly: the case of an infinitely thin crack. The problem is then much simpler since only the crack tip velocity (and not the crack geometry) remains unknown. It is determined by the condition of consistency of the electric potential and the temperature field. In this geometry, the electric problem (16a)–(16c) can be solved exactly, as shown in Appendix B. Reporting this solution in Eq. (19) with  $T=1$  then yields the crack tip velocity  $U$ . The solution of this special case is shown in Appendix B.

There is another limit which allows for an explicit treatment and which turns out to recover exactly the continuum of solutions of the Saffman-Taylor problem (17) (see Appendix A). Let us consider the limit where the front velocity  $U$  is small. By small, we mean that the term  $U\partial T/\partial x$  can be neglected compared to the two other terms in the right hand side of Eq. (16d). This implies that the temperature is always equal to

$$T = a^{-1}G^{m-1}/|\nabla\Phi|^m \quad (20)$$

everywhere. The crack boundary is thus given by the condition (16f)  $a^{-1}G^{m-1}|\nabla\Phi|^m=1$  where  $\nabla\Phi$  must be evaluated on the crack boundary. Since  $\partial\Phi/\partial n=0$  on the crack boundary according to (16c), then  $|\nabla\Phi|=\partial\Phi/\partial s$ , where  $s$  is the curvilinear abscissa of the crack border, whose origin is conveniently taken at the tip. This means that the equation of the crack border is

$$\partial\Phi/\partial s = aG^{1-m} \equiv V', \quad (21)$$

i.e., the crack frontier corresponds to a constant  $\partial\Phi/\partial s$ . Note that  $V'$  has the physical dimension of a voltage in the units where the strip width extends from  $-1$  to  $+1$ . Equation (21) yields  $\Phi=V's$ , with our choice of origin. Sufficiently close to the tip such that  $\partial\Phi/\partial s \approx \partial\Phi/\partial y$  for  $\cos\phi \approx 1$ , where  $\phi$  is the angle between the normal of the border and the  $Ox$  axis, one has  $\Phi \approx V'y$ , which corresponds exactly to the Saffman-Taylor solution (see Appendix A). Thus the shape of the cracks is close to the fingers of the Saffman-Taylor problem in the region where the frontier is approximately vertical, i.e., sufficiently close to their tips. Further away, their shapes depart from the Saffman-Taylor fingers. Indeed, from  $\Phi=V's$  and since  $\Phi \leq V$ , this means that  $s$  must be finite, i.e., the length of the crack frontier should be finite. In other words, this does not give a fingerlike shape extending to  $-\infty$ , but rather to a front which connects to the two bus bars at a finite distance from the tip. This conclusion is valid as long as the conditions for neglecting the term  $U\partial T/\partial x$  hold. The connection of the crack to the two bus bars must thus occur with a sufficiently large angle so that  $|U\partial T/\partial x|$  remains smaller than

$G^{m-1}|\nabla\Phi|^m$ , this last term going to zero as the angle  $\phi$  (defined in Fig. 7) goes to  $\pi/2$ . Note also that this solution involves a rather special continuum limit. Indeed, suppose that one starts from a discrete lattice of mesh size  $\Delta x$ . For the term  $U\partial T/\partial x$  to be small compared to the first term on the right hand side of Eq. (16d),  $U$  is less than  $a\Delta x$ , where  $a^{-1}$  is the thermal relaxation time introduced by the coupling with the thermal bath. When taking the continuous limit ( $\Delta x \rightarrow 0$ ) leading to Eqs. (16), we have to look for very slowly propagating cracks such that the limit  $\Delta x \rightarrow 0$  is taken while keeping the condition  $U < a\Delta x$ . When this condition holds, the relaxation of the temperature is sufficiently fast such that at all times one can neglect the term  $U\partial T/\partial x$  in Eq. (16d) compared to the first term on the right hand side of Eq. (16d).

It is interesting to note that we would recover exactly the Saffman-Taylor solution, for  $U \rightarrow 0$ , if Eq. (16d) is replaced by

$$-U\partial T/\partial x = G^{m-1}|\partial\Phi/\partial y|^m - aT, \quad (22)$$

i.e., by replacing  $|\nabla\Phi|$  by  $\partial\Phi/\partial y$  in Eq. (16d). In the discrete-continuum correspondence, Eq. (22) corresponds to heating only the vertical bonds along the  $Oy$  axis, which are parallel to the globally applied voltage gradient. This condition could perhaps find a physical interpretation within an extension of the present scalar rupture model to a tensorial formulation. In any case, this formulation (22) simplifies the analysis considerably, since with the quasistatic assumption, it leads to replacing Eq. (21) by

$$\partial\Phi/\partial y = aG^{1-m} \equiv V'. \quad (23)$$

This gives exactly the Saffman-Taylor solution, since upon integration we get  $\Phi=V'y$  on the crack border (see Appendix A). Note that the half-width  $\lambda$  of a crack is given by  $\lambda=V/V'$  because the potential  $\Phi$  reaches its limit  $V$  for  $x \rightarrow -\infty$  and  $y=\lambda$ . Therefore  $V'$  must be larger than or equal to  $V$  in order for a solution to exist. However, contrary to the Saffman-Taylor finger problem,  $V'$  does not give the velocity of the front, which is in our case infinitely small. This is where the duality of the two problems makes them different.

Putting aside the technical aspects of the analytical treatment and the various limits, the important result is that the solution of the set of Eqs. (16), defining the continuous limit of the crack front propagation in a strip under constant voltages (displacements) applied at the borders, is not unique but rather corresponds to a continuum of solutions of different shapes parametrized by their corresponding velocity  $U$ . This result is completely analogous to the problem of the penetration of a single finger of light fluid penetrating in a denser fluid in a channel, in the limit of vanishing surface tension. It is also similar to the problem of the growth of a dendrite in a capillary also in the absence of surface tension and to the propagation of a retrocombustion front in a plate of wood in which an oxygen flow is injected at one extremity and combustion is initiated at the other [6]. In all cases, the existence of the continuum family of solutions can be traced back to the fact that the front boundary is coinciding with the isovalue of the relevant field. In the Saffman-Taylor

finger, the border is an isopressure line, and therefore an isopotential taking into account Darcy's law. In the dendrite problem, the border is an isotherm line and in the retrocombustion it is again an oxygen isopressure line. In our electrical thermal fuse (mechanical damage) problem, the crack border corresponds to an isotherm (isodamage) line.

The existence of a small surface tension in the Saffman-Taylor finger, the dendrite, or the retrocombustion problems leads to the selection of one shape among all of the continuous family of solutions [16]. The surface tension implies physically that the fronts are no longer isovalues of the relevant field. A similar effect should hold for the rupture problem. A possible effect would be to consider both damage and plasticity such that the deformation is no longer purely elastic and the crack border is defined by combining plastic deformation and damage in a rupture criterion. We leave this problem for future investigations.

## V. DISCUSSION

The thermal fuse model of dynamical rupture has been shown to possess many properties in common with other general surface growth phenomena. In ordered or in slightly disordered lattices under constant applied density current, dendritic patterns have been obtained which correspond to a selective amplification of very small noisy fluctuations on the side of the cracks. We would like to point out that the crack patterns, grown from a nucleation center in the presence of quenched disorder which are observed in our computations, are reminiscent of recent high velocity fluid-displacement experiments in Hele-Shaw cells filled with a viscoelastic fluid [18]. In these experiments, the role of the nucleation center is played by the injection hole through which the fluid is pushed in and the quenched disorder accounts for the heterogeneities of the system. Even if the physics may be more complicated in the experiments, the existence of viscoelasticity entails delay and relaxation effects as in the thermal fuse model. More generally, the addition of a dynamics with delay and relaxation effects creates a very rich phenomenology similar and sometimes close to real-life observations of rupture patterns. The present model constitutes one of the simplest realizations of dynamical systems exemplifying the importance of viscoelastic, ductile, or plastic behavior coupled with the usual linear elasticity on rupture phenomena.

We speculate that the existence of the continuum of solutions (Sec. IV) found in the continuous version of the thermal fuse model, of a crack front propagating at a constant velocity in a strip on whose borders constant displacements are applied, could be related to the accumulation of instabilities which have been observed numerically in Sec. III when  $m$  approaches 1 for the problem of crack growth from a central nucleus under constant applied stress. The idea is that the continuum set of solutions provides a large set of almost equivalent shapes which can compete in the rupture dynamics. We do not understand precisely the status of the apparently special value  $m=1$ , but note that integration of Eq. (1) (for

$m=1$  and  $a=0$  or  $a\neq 0$  but for large applied currents) yields that rupture occurs on a given element after a time such that the integrated current over this time reaches a constant, characteristic of this element. Since the integrated current is simply proportional to the electric charge accumulated over this time, the rupture criterion boils down to a threshold criterion on the electric charge having passed through that element. The special value  $m=1$  then stems from the fact that rupture criterion is expressed in terms of a conserved quantity of the driving field, namely, the electric charge. It can then be shown [9] that the average time to failure is proportional to the length (in a certain metric) of the shortest path cutting the system into two pieces. In this case, there is a clear geometrical interpretation to the fractal and scaling behaviors close to rupture: it is related to the geometrical structure of minimal paths in a certain metric.

We have attempted to complement the theoretical analysis developed in Sec. IV by performing extensive numerical computations on large lattices (size up to 100 by 500). We were hoping that, for these large lattices, the discreteness would not be too severe a perturbation and that the cracks would present shapes close to the expected continuous solutions, at least for low velocities (and possibly  $m\rightarrow 0$ ). In particular, we wanted to check our prediction that the shape of the crack front could be selected in a large family of possible solutions, by controlling the width and shape of the initial crack. We also wanted to check the prediction that the shapes of these crack fronts are close to those of the Saffman-Taylor fingers in the vicinity of the tip, for low velocities. These expectations have not been borne out by our numerical simulations. In fact, we found our simulation not very reliable for two reasons: (1) due to the finite length of the strip, it is almost impossible to start the simulation with the correct asymptotic temperature field. In other words, the crack solution is sensitive to the initial temperature field and the various structures of the cracks found numerically reflect this fact. (2) The results were found to be very sensitive to the initial set of bonds removed, i.e., to the initial shape of the crack. Using square lattices tilted at  $45^\circ$  and square lattices not tilted with respect to the long direction of the strip and a large variety of initial shapes (sometimes forcing the shape close to the expected continuous shape), we found that thin cracks were almost always preferred, with possibly rather complicated trajectories between the two strip edges. The main conclusion of this numerical work is that discreteness is a relevant singular perturbation whose effects are too important to get access to the continuum solutions. This is basically due to the preferred crack growth along the direction of the largest current. The situation thus appears similar to the case of dendritic growth where the underlying crystal structure is very important [7]. Note that this is similar to the viscous fingering problem in which rules mimicking surface tension had to be added to the DLA walkers to get appropriate continuum behavior. One could add similar smoothing terms, such as a coupling between damage and plasticity such that the deformation is no longer purely elastic and the crack border is defined by combining plastic deformation and damage in a rupture

criterion. Another possibility would be to consider a diffusion of damage (heat) to neighboring sites; however, this has no physical basis and would destroy the simplicity of the present model which couples the damage field to the stress field only locally through Eq. (1).

Inspired by our results described in Sec. III for small exponents  $m$ , we then attempted to get a Saffman-Taylor-like crack front in the regime of accelerating cracks (regime [(1)ii] of Sec. II C), by applying a large voltage  $V$  at time zero to the bus bars of the strip. In these simulations, the temperature of all bonds is zero at the initial time. The results found are quite intriguing: fixing first the exponent  $m$  to a small value, we find a fingerlike solution for the crack front, with a rather smooth tip. Its thickness  $\lambda$  is smaller than  $\frac{1}{2}$  the strip thickness, namely,  $\lambda < 1$ , using the notation of Fig. 7. However,  $\lambda$  increases monotonously as the applied volt-

age increases to infinity and eventually saturates to a value less than 1. Decreasing  $m$  to very small values (down to  $10^{-5}$ ) and applying very large voltage (up to  $10^{10}$ , where 1 corresponds in these units to the rupture threshold  $V_{th}$  defined in Sec. III C), we find that  $\lambda \rightarrow 1$ , i.e., the crack front has its width converging to half the strip width, while its shape becomes close to the Saffman-Taylor solution for this value (up to the resolution of the discrete lattice). Figure 8 illustrates these results, for  $m = 10^{-5}$  and  $V = 10^{10}$ , by showing a series of snapshots of the crack front developing from an initial small crack into a well-defined finger of width equal to 24 lattice mesh (the entire width is 49), very close to the asymptotic value. This selection of a well-defined width converging to half the strip width for infinitesimal  $m$ 's and infinite  $V$ 's is quite intriguing since this is the solution of the Saffman-Taylor problem in the presence of a

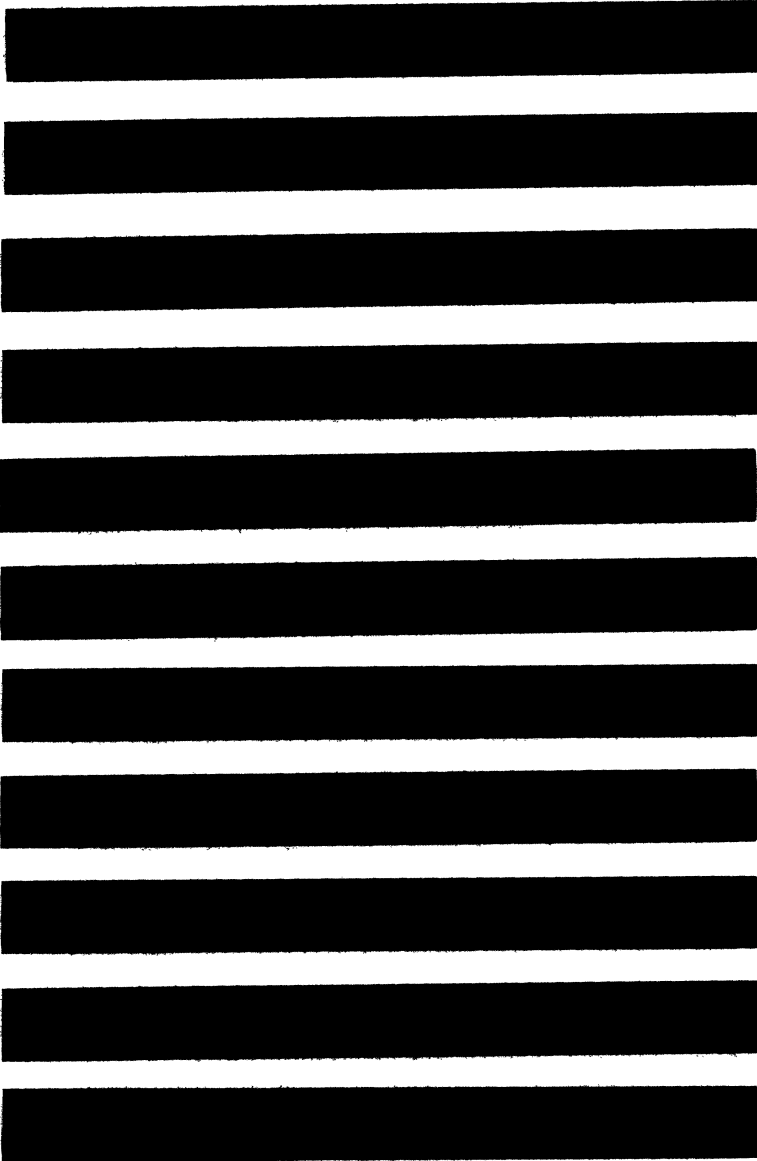


FIG. 8. For  $m = 10^{-5}$ ,  $V = 10^{10}$ , and periodic boundary conditions in the  $x$  variable, series of snapshots showing the crack front developing from an initial small crack into a well-defined finger of width equal to 24 lattice meshes (the strip shown in the figure has a length of 512 meshes and a width of 49 meshes), very close to the asymptotic value of half the strip width. Only half of the strip is used in the calculation, due to symmetry with respect to the  $Ox$  axis. The succession of snapshots corresponds to the following number of broken bonds: 100, 300, 500, 1000, 1500, 2000, 3000, 5000, 6000, 8000, 9500.

small surface tension [16]. In this last case, the shape and corresponding velocity selection are due to a solvability principle in the presence of the essential singularity provided by the presence of the small surface tension [16]. In the present case, however, the front crack is not a steady-state solution since it is accelerating and a mathematical correspondence, if any, is not clear to us.

#### ACKNOWLEDGMENTS

We acknowledge very stimulating discussions with B. Derrida and A. Karma. D. S. thanks the Institute for Theoretical Physics, University of California, Santa Barbara, for its hospitality, where part of this work was done. This work was partially supported by NSF Grant No. PHY89-04035.

#### APPENDIX A: SOLUTION OF THE ELECTRIC BOUNDARY PROBLEM [EQS. (16a)–(16c)]

The general method for solving the crack propagation problem is the following. We use the change of variables  $x, y \rightarrow \Phi, \Psi$  formulated below. We use the form (A4) below for  $y(\Phi, \Psi)$  which gives  $x(\Phi, \Psi)$ , using the Cauchy relations  $\partial x / \partial \Phi = \partial y / \partial \Psi$  and  $\partial x / \partial \Psi = -\partial y / \partial \Phi$ . This change of variables  $x, y \rightarrow \Phi, \Psi$  allows us to express Eq. (19) on the crack boundary where  $T=1$ , in terms of the variables  $\Phi, \Psi$ , which thus yields the equation of the crack as a relation between  $\Phi$  and  $\Psi$ . Using it and the transformation  $x, y \rightarrow \Phi, \Psi$  allows us to compute the current density  $\partial \Phi / \partial s$  along the crack boundary from which one can extract the dependence of the electric potential  $\Phi_B(s)$  on the crack boundary and thus the relation giving  $y$  as a function of  $\Phi$  (which constitutes a way to write the equation of the crack boundary, since  $\Psi=0$  on it),  $y_B(\Phi)$ , using the relation between  $y$  and the curvilinear abscissa  $s$ . Then, Eq. (A5) below provides the unknown Fourier coefficients  $A_n$  from which all other quantities are obtained. We expect a continuum of solutions, each solution being parametrized by its corresponding velocity  $U$ . What this means is that, fixing  $0 \leq U \leq +\infty$  in Eqs. (16), one can always find a shape for the crack boundary which is a solution of (16). We have not been able to follow this program in order to find an explicit analytical solution, similarly to the Saffman-Taylor solution of Eqs. (17). The crack shape and its velocity can only be solved numerically.

We now expose the procedure in more detail. The method of resolution is similar to that used to solve the Saffman-Taylor problem. One introduces first the "stream function"  $\Psi$  defined by

$$\partial \Phi / \partial x = \partial \Psi / \partial y, \quad (\text{A1a})$$

$$\partial \Phi / \partial y = -\partial \Psi / \partial x. \quad (\text{A1b})$$

Then the condition (16c),  $\partial \Phi / \partial n|_{y=\pm f(x)}=0$ , becomes  $\Psi|_{y=\pm f(x)}=0$  using the fact that  $\partial \Phi / \partial n = \partial \Psi / \partial s$  [from the definition (A1)], where  $s$  is the curvilinear abscissa along the crack boundary. The variable  $\Psi$  is thus a constant along the crack boundary, which can be taken zero without loss of generality.

Instead of looking for a solution  $\Phi$  and  $\Psi$  as a function

of  $(x, y)$  the trick is to consider  $x + iy$  as an analytic function of  $\Phi + i\Psi$ , where  $\Phi$  and  $\Psi$  are now the plane variables. The  $(x, y)$  plane transforms into the  $(\Phi, \Psi)$  shown in Fig. 9 with the corresponding boundary conditions. What we gain in this transformation is the fact that the unknown crack boundary becomes the  $GA$  segment on the  $\Phi$  axis ( $\Psi=0$ ). The interior of the strip is now the infinite strip  $EFBC$ . We have the following boundary conditions:

$$y(\Phi = \pm V, \Psi) = \pm 1$$

$$\text{(imposed potential on the two bus bars),} \quad (\text{A2a})$$

$$y(\Phi = 0, \Psi) = 0$$

$$\text{(symmetry with respect the } 0x \text{ axis).} \quad (\text{A2b})$$

In the Saffman-Taylor problem (17), an additional condition is easily obtained from the local growth law condition (17d). In the crack context (16), this would read

$$y = \Phi / V' \text{ on the finger boundary for which } \Psi = 0.$$

$$(\text{A3})$$

This condition would hold if  $\partial \Phi / \partial s = V' \cos \phi$ , which is the dual of Eq. (17c) for the Saffman-Taylor problem, where  $V'$  is the maximum current density at the crack tip, for a conductivity equal to unity. Using  $\cos \phi = \partial y / \partial s$ , this yields (A3) upon integration. Unfortunately, the solution is not as easy in the case of Eqs. (16), since  $\partial \Phi / \partial s$  is not in general proportional to  $\cos \phi$ . A possible formulation is to replace the crack boundary geometry by the function  $j(s)$  giving the current density along its border. From  $j(s) = G \partial \Phi / \partial s$ , this yields  $\Phi_B(s)$  on the crack boundary and thus  $y_B(\Phi)$  using the relation between  $y$  and the curvilinear abscissa  $s$ .

This is a general fact that  $y$  is a harmonic function of  $\Phi$  and  $\Psi$  which can thus be looked for under the form

$$y = \Phi / V + \sum_{n=1}^{+\infty} A_n \sin(n\pi\Phi/V) \exp\{-n\pi\Psi/V\}. \quad (\text{A4})$$

The term  $\Phi/V$  ensures that we recover the solution  $\Phi = Vy$  for  $x \rightarrow +\infty$ , i.e.,  $\Psi \rightarrow +\infty$ . Suppose that we know  $y_B(\Phi)$  on the crack boundary on which  $\Psi=0$ .

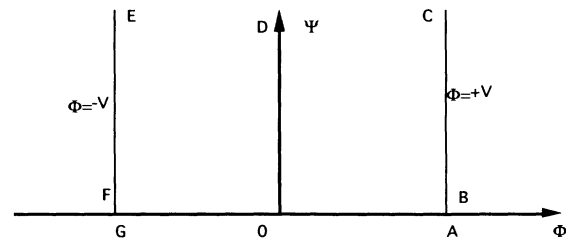


FIG. 9. Plane  $(\Phi, \Psi)$ . Corresponding points in the physical and potential planes are marked with the same letter (see Fig. 7), the exterior of the crack transforms into the semi-infinite strip  $\Psi > 0$ ,  $-V < \Phi < V$ , the surface of the crack transforms into the  $\Phi$  axis with  $-V < \Phi < V$ , and the walls of the strip correspond to the semi-infinite lines  $\Phi = \pm V$ .

Then, the equation

$$y_B(\Phi) = \Phi/V + \sum_{n=1}^{+\infty} A_n \sin(n\pi\Phi/V) \quad (\text{A5})$$

means that the coefficients  $A_n$  are simply the Fourier coefficient of the function  $y_B(\Phi)$  defined in the finite interval  $-V \leq \Phi \leq V$ . This equation ensures that all the boundary conditions are satisfied. Knowing the  $A_n$ 's, we then deduce  $x(\Phi, \Psi)$  and  $y(\Phi, \Psi)$ , from which we can extract  $\nabla\Phi$  and report this value in the thermal equations (16d) and (16f).

Note that if Eq. (A3) held ( $y = \Phi/V'$ ) on the finger boundary for which  $\Psi = 0$ , we would recover the Saffman-Taylor solution [with, however, a permutation between  $\Phi$  and  $\Psi$  coming from the dual boundary condition (16c) compared to (17c)]:

$$A_n = -(2/\pi)(1 - V/V'), \quad (\text{A6})$$

which would solve completely the problem [6], assuming a conductivity equal to unity. The constant  $V'$  is such that  $V \leq V'$  is not fixed and this means that there is a continuum of solutions parametrized by the ratio  $0 \leq \lambda = V/V' \leq 1$ , where  $\lambda$  has a simple geometrical meaning, being the half-width of the finger, as seen from Eq. (A3)  $y = \Phi/V'$ , since  $\Phi$  must reach its limit  $V$  for  $y = \lambda$ .

#### APPENDIX B: INFINITELY THIN CRACK CASE

We want to solve the set of Eqs. (16) with the additional assumption that the crack is given *a priori* and takes the shape of a line equation  $y=0$ ,  $-\infty < x \leq 0$ . Then, condition (16c) becomes  $\partial\Phi/\partial y = 0$  since the normals to the crack are always parallel to the  $Oy$  axis. The half-width  $\lambda$  of the crack is vanishing. Since in the Saffman-Taylor problem (see Appendix A) it is given as the ratio  $\lambda = V/V'$  where  $V'$  is defined by the relationship linking the potential  $\Phi$  on the crack border to the variable  $y$ , this gives  $V' \rightarrow +\infty$ . Another way to put it is that  $\Phi$  must go to  $V$  for  $x \rightarrow \infty$ ,  $y = 0$ . We can thus use the method sum-

marized in Appendix A and write the solution for the potentials  $\Phi$  and  $\Psi$  as follows, taking  $\lambda = 0$  [6]:

$$x = \frac{\Psi}{V} + \frac{2}{\pi} (\ln 2 + \frac{1}{2} \ln \{ [1 + e^{-\pi\Psi/V} \cos(\pi\Phi/V)]^2 + [e^{-\pi\Psi/V} \sin(\pi\Phi/V)]^2 \} ), \quad (\text{B1})$$

$$y = \frac{\Phi}{V} - \frac{2}{\pi} \frac{e^{-\pi\Psi/V} \sin(\pi\Phi/V)}{1 + e^{-\pi\Psi/V} \cos(\pi\Phi/V)}. \quad (\text{B2})$$

Eliminating  $\Psi$  between these two equations allows us to obtain the potential  $\Phi$  as a function of  $x$  and  $y$ .

In order to solve for the crack tip velocity, we need to determine the current flowing on the line  $y=0$ ,  $x \geq 0$ . For symmetry reasons, this current is vertical and is given by  $\partial\Phi/\partial y|_{y=0} = 0$ . Since  $\Phi(y=0) = 0$ , this allows us to obtain  $\Psi(x)$  from Eq. (B1) on the line  $y=0$ :

$$x = \frac{\Psi}{V} + \frac{2}{\pi} \{ \ln 2 + \ln(1 + e^{-\pi\Psi/V}) \}. \quad (\text{B3})$$

Using the Cauchy relation  $\partial\Phi/\partial y = -\partial\Psi/\partial x$ , we obtain the current needed in Eq. (19) and setting  $T=1$ , which defines the frontier of the crack, we get the implicit equation

$$U = (GV)^{m-1} \int_0^{+\infty} \left| \frac{1 + e^{-\pi\Psi/V}}{1 - e^{-\pi\Psi/V}} \right|^{m-1} e^{-a\Psi/UV} \times \left[ \frac{1 + e^{-\pi\Psi/V}}{2} \right]^{-2a/\pi U} d\Psi, \quad (\text{B4})$$

which gives the velocity  $U$  as a function of the applied potential  $V$ . Note that  $U$  appears in the integrand of the integral. The absolute value in the integral is  $\partial\Phi/\partial y$ , the exponent  $m=1$  coming from the correction brought by the Jacobian of the transformation  $x \rightarrow \Psi$  and the two other terms are the expression of  $e^{-ax/U}$  in terms of the variable  $\Psi$ , using Eq. (B3). This solves formally the problem of the determination of the crack tip velocity.

- 
- [1] (a) D. Sornette and C. Vanneste, *Phys. Rev. Lett.* **68**, 612 (1992); (b) C. Vanneste and D. Sornette, *J. Phys. I* **2**, 1621 (1992); (c) D. Sornette, C. Vanneste, and L. Knopoff, *Phys. Rev. A* **45**, 8351 (1992).
- [2] See, e.g., *Statistical Models for the Fracture of Disordered Media*, edited by H. J. Herrmann and S. Roux (Elsevier, Amsterdam, 1990).
- [3] *Disorder and Fracture*, Vol. 235 of *NATO Advanced Study Institute, Series B: Physics*, edited by J. C. Charvet, S. Roux, and E. Guyon (Plenum, New York, 1990).
- [4] See, e.g., *On Growth and Form*, edited by H. E. Stanley and N. Ostrowsky (Kluwer, Boston, 1986).
- [5] H. J. Herrman, J. Kertész, and L. de Arcangelis, *Europhys. Lett.* **10**, 147 (1989).
- [6] P. Pelcé, *Dynamics of Curve Fronts* (Academic, Boston, 1988).
- [7] *Growth and Form, Nonlinear Aspects*, edited by M. Ben Amar, P. Pelcé, and P. Tabeling (Plenum, New York, 1991).
- [8] R. C. Ball and R. Blumenfeld, *Phys. Rev. Lett.* **65**, 1784 (1990); R. C. Ball, P. W. Barker, and R. Blumenfeld, *Europhys. Lett.* **16**, 47 (1991); R. Blumenfeld and R. C. Ball, *Physica A* **177**, 407 (1991).
- [9] R. M. Bradley and K. Wu, *J. Phys. A* **27**, 327 (1994); *Phys. Rev. E* **50**, 631 (1994).
- [10] K. Aki and O. G. Richards, *Quantitative Seismology, Theory, and Methods* (Freeman, San Francisco, 1980), Vol. II, p. 833.
- [11] L. M. Kachanov, *On the Problem of Propagation of Cracks Under Conditions of Creep, in Problems of Hydrodynamics and Continuum Mechanics, Contributions in Honor of the Sixtieth Birthday of Academician L. I. Sedov* (Society for Industrial and Applied Mathematics, Philadelphia, 1969).
- [12] See, for instance D. Krajcinovic and J. Lemaitre, *Continuum Damage Mechanics: Theory and Applications, CISM Course* (Springer-Verlag, Berlin, 1987); L. M. Kachanov, *Introduction to Continuum Damage Mechanics* (Nijhoff, Amsterdam, 1986).

- [13] C. Vanneste, A. Gilbert, and D. Sornette, *J. Phys. A* **23**, 3591 (1990).
- [14] R. Pieters and J. S. Langer, *Phys. Rev. Lett.* **56**, 1948 (1986); J. S. Langer, in *Lectures in the Theory of Pattern Formation, in Chance and Matter, Les Houches Session XLVI*, 1986, edited by J. Souletie, J. Vannimenus, and R. Stora (North-Holland, Amsterdam, 1987); D. Bensimon, L. P. Kadanoff, S. Liang, B. I. Shraiman, and C. Tang, *Rev. Mod. Phys.* **58**, 977 (1986).
- [15] M. Barber, J. Donley, and J. S. Langer, *Phys. Rev. A* **40**, 366 (1989).
- [16] R. Combescot, V. Hakim, T. Dombre, Y. Pomeau, and A. Pumir, *Phys. Rev. A* **37**, 1270 (1988).
- [17] Note that a simple analytical solution of this problem has been possible due to the small width of the strip equal to three lattice meshes. This finite size changes the long-range  $r^{-1}$  electric current Green function into a short-range exponentially decaying Green function, with a characteristic decay length equal to  $[\ln(s_5 - 1)]^{-1} \approx 0.64$  lattice mesh. In strips of increasing width  $L$ , the decay length of the Green function increases linearly with  $L$ : this constitutes a simple example of finite size scaling [see, for instance, J. L. Cardy, *Finite Size Scaling, Current Physics, Sources, and Comments* (North-Holland, Amsterdam, 1988)].
- [18] E. Lemaire, P. Levitz, G. Daccord, and H. Van Damme, *Phys. Rev. Lett.* **67**, 2009 (1991).

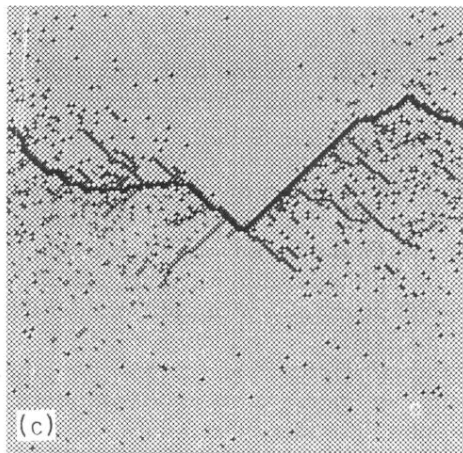
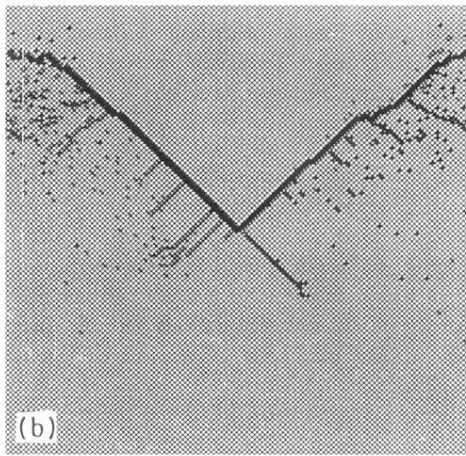
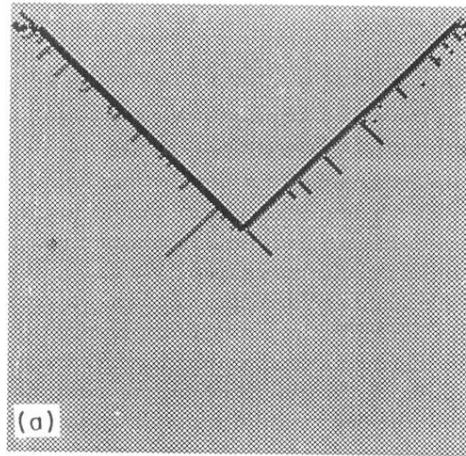


FIG. 1. Typical crack patterns at the final stage of rupture in a square lattice of size 180 by 180 tilted at 45°. The conductances are uniformly sampled in the interval [0.9,1.1]. The three pictures correspond to exactly the same disorder realization with, however, different applied currents. (a) Regime close to the rupture threshold:  $I \approx I_c = 0.913$ ; (b) intermediate regime  $I = 1$ ; (c) asymptotic regime  $I = 30 (\gg I_c)$ .

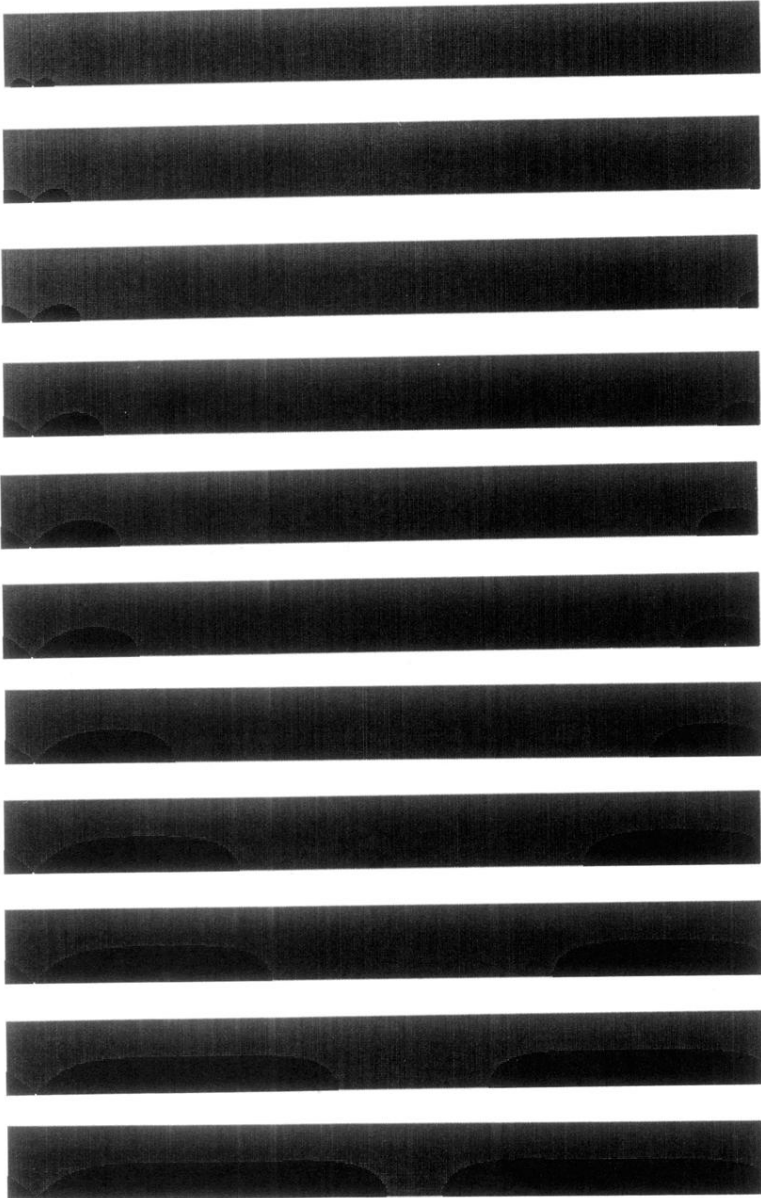


FIG. 8. For  $m = 10^{-5}$ ,  $V = 10^{10}$ , and periodic boundary conditions in the  $x$  variable, series of snapshots showing the crack front developing from an initial small crack into a well-defined finger of width equal to 24 lattice meshes (the strip shown in the figure has a length of 512 meshes and a width of 49 meshes), very close to the asymptotic value of half the strip width. Only half of the strip is used in the calculation, due to symmetry with respect to the  $Ox$  axis. The succession of snapshots corresponds to the following number of broken bonds: 100, 300, 500, 1000, 1500, 2000, 3000, 5000, 6000, 8000, 9500.